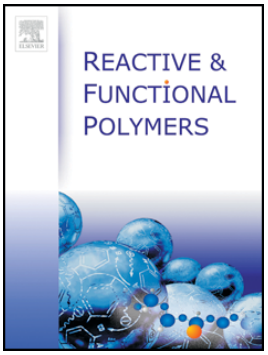

Bionanostructure-catalyzed one-pot three-component synthesis of 3,4-dihydropyrimidin-2(1H)-one derivatives under solvent-free conditions

Ali Maleki, Reza Paydar

PII: S1381-5148(16)30207-3
DOI: doi:10.1016/j.reactfunctpolym.2016.10.013
Reference: REACT 3765

To appear in:

Received date: 3 February 2016
Revised date: 16 October 2016
Accepted date: 31 October 2016

Please cite this article as: Ali Maleki, Reza Paydar, Bionanostructure-catalyzed one-pot three-component synthesis of 3,4-dihydropyrimidin-2(1H)-one derivatives under solvent-free conditions, (2016), doi:10.1016/j.reactfunctpolym.2016.10.013

ELSEVIER

Reactive and Functional Polymers

www.sciencedirect.com

Bionanostructure-catalyzed one-pot three-component synthesis of 3,4-dihydropyrimidin-2(1H)-one derivatives under solvent-free conditions

Ali Maleki * and Reza Paydar

Catalysts and Organic Synthesis Research Laboratory, Department of Chemistry, Iran University of Science and Technology, Tehran 16846-13114, Iran

**Corresponding author. Tel.: +98 21 77240640-50; Fax: +98 21 73021584. E-mail: maleki@iust.ac.ir (A. Maleki).*

ARTICLE INFO

Article history:
Received
Received in revised form
Accepted
Available online

Keywords:
Bionanocatalyst
Chitosan
Dihydropyridinones
Graphene oxide
Multicomponent reactions

ABSTRACT

In this work, chitosan/graphene oxide as a green bionanocomposite catalyst was synthesized and characterized by Fourier transform infrared spectroscopy (FT-IR) spectra, thermal gravimetric analysis (TGA), differential scanning calorimetry (DSC) analysis, atomic force microscopy (AFM) and scanning electron microscopy (SEM) images. Then, it was used as a nanocatalyst for the synthesis of 3,4-dihydropyrimidin-2(1*H*)-one derivatives by a one-pot three-component condensation reaction of benzaldehyde, 1,3-ketoesters and urea in excellent yields and short reaction times under solvent-free conditions. The reaction work-up was simple and the catalyst could easily be separated from the reaction mixture and reused in subsequent reactions.

1. Introduction

In comparison with classical stepwise strategies in organic synthesis, multicomponent reactions (MCRs), as processes in which three or more materials compose to yield a product, have many advantages and properties such as synthesizing of various products with different molecular structures in brief reaction time, saving money, crude materials and so on. MCRs have represented a rapid and easy access to biologically relevant and pharmaceutical compounds as a preferred method to design and discover these compounds [1].

In recent years, dihydropirimidines (DHPMs) have attracted much attention due to their interesting biologically activities and properties. Pharmaceutical applications of multifunctionalized DHPMs are significant such as using for the synthesis of antiviral, antitumor, antibacterial and antiinflammatory drugs [2,3]. Recently, many catalysts for the Biginelli reaction and synthesis of DHPMs have been introduced to improve the synthesis of this attractive family of compounds such as: 2-oxo-2-polyfluoroalkylethane-1-sulfones and –sulfamides [4], phytic acid [5], nanomagnetic-supported sulfonic acid [6], 1-glycyl-3-methyl imidazolium chloride copper(II) complex [7], pyridine dicarboxylic acid guanidine–cobalt complex (PDAG-Co) [8], carbon nanotubes supported by titanium dioxide nanoparticles [9], cerium(III) trislaurylsulfonate ($Ce(LS)_3$) [10], solid acidcatalysts [11], trimethylsilyl chloride (TMSCl) [12], solid silica-based sulfonic acid [13], silica-bonded *N*-propyl sulfamic acid [14], magnetic nanoparticles supported imidazolium-based ionic liquids [15], molybdenum oxide nanoparticle [16], gallium nafionate [17], phosphonic acid functionalized ordered mesoporous material [18], phthalimide-*N*-sulfonic acid [19], diaryliodonium salts [20], Fe_3O_4–MWCNT nanocomposite [21] and ZrO_2–Al_2O_3–Fe_3O_4 [22]. However, most of these catalytic methodologies suffer from overwhelming drawbacks like long reaction time, low yield, high reaction temperature, metal leaching and solubility of the catalyst in the reaction medium.

Recently, paying attention to design and development of green catalysts and catalytic processes and consequently greener reaction pathways and methodologies have been increased [23]. In this context, in connection with our previous works [24, 29], we want to introduce a metal-free organocatalyst as a green catalytic methodological approach in the field of synthetic organic chemistry to improve the reaction conditions.

Graphene and graphene oxide (GO) are novel nanomaterials [30] that have significant applications in nanoelectronics [31], sensors [32], nanocomposites [33], batteries [34], supercapacitors and energy storage [35]. In recent years, there has been a rush of interest in functionalizing GO materials with various polymers and biopolymers for various applications [24].

Chitosan, as a natural polymer, has attracted considerable attention due to its unique properties [36, 37]. It also has several chemical, medicinal and industrial applications [38]. Accordingly, functionalization of GO with chitosan for reaching the exceptional properties of both materials could be of prime importance. Accordingly, we have considered GO-chitosan as a green nanocatalyst for the synthesis of multifunctionalized DHPMs **4a-s**, by a one-pot MCR of various benzaldehydes **1**, 1,3-ketoesters **2** and urea **3** at 110 °C under solvent-free conditions (Scheme 1).

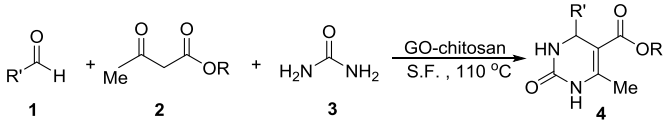

Scheme 1. GO-chitosan catalyzed synthesis of DHPMs **4a-s**.

2. Results and discussion

FT-IR spectroscopy was used to study and comparison the bonds of GO-chitosan with GO and chitosan (Figure 1). In the IR spectrum of GO, the peak at 1739 cm^{-1} is attributed to the C=O bonds of carbonyl and carboxyl groups. In the IR spectrum of chitosan, the peak at 1593 cm^{-1} is attributed to the C=O bonds of NHCO. In the spectrum of GO–chitosan, the peak located at 1594 cm^{-1} is attributed to the C=O bonds of NHCO and the peak at 1038 cm^{-1} is attributed to the N–H bending of NH_2. Furthermore, the peak at 1739 cm^{-1} that is present in the IR spectrum of GO which indicates the C=O bonds of carboxylic acids and other carbonyl groups, is absent in the IR spectrum of GO–chitosan, which means the mass ratio of GO to chitosan is 1:9 [39].

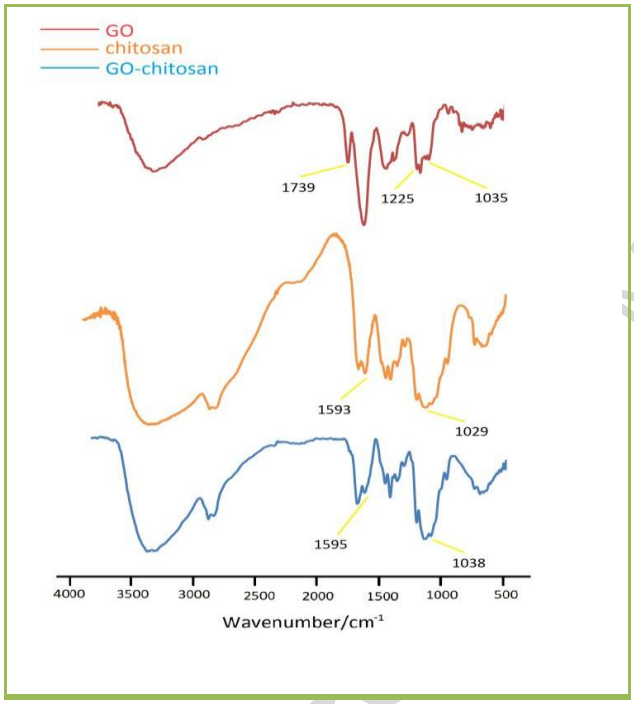

Figure 1. FT-IR spectra of GO, chitosan and GO-chitosan.

Thermal properties of the nanocomposite were investigated by thermal gravimetric analysis (TGA) and differential scanning calorimetry (DSC). Thermal stability of GO-chitosan is significantly better than GO and chitosan. As shown in Figure 2, in GO-chitosan no significant loss of mass is seen even at 300 °C.

Another evidence for the thermal properties improvement of GO-chitosan in comparison to chitosan is the glass transition temperatures (T_g) that is obtained from differential scanning calorimetry (DSC) (Figure 3). The glass transition occurs at 116-118 °C for pristine chitosan, while it shifts to 162 °C for GO-chitosan composites. Since our reaction is done at high temperature, GO-chitosan for having better thermal properties is the best choice as a catalyst.

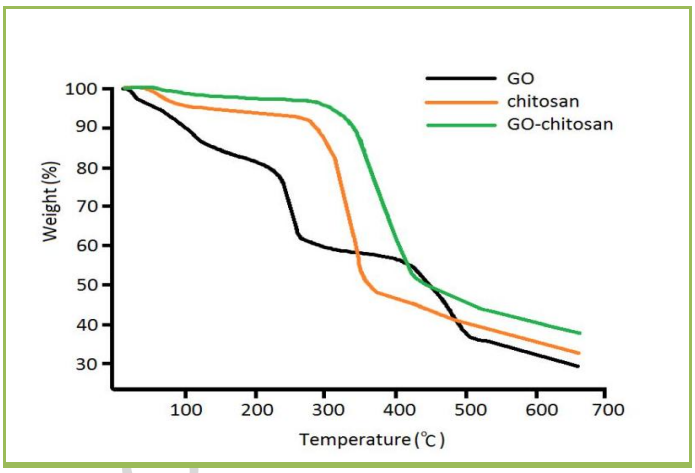

Figure 2. TGA analysis of GO, chitosan and GO-chitosan.

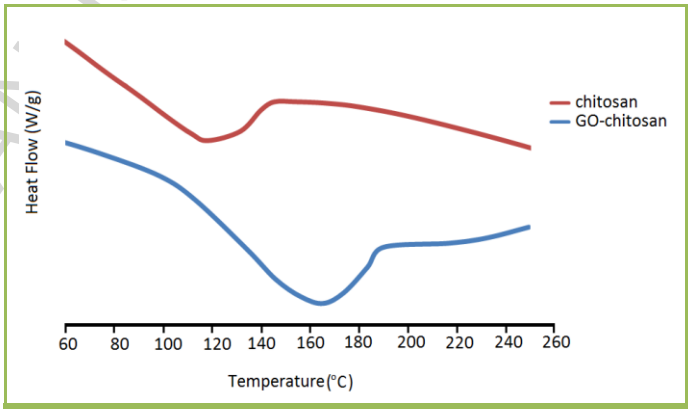

Figure 3. DSC analysis of GO, chitosan and GO-chitosan.

To determine the morphology of GO-chitosan nanocomposite, scanning electron microscopy (SEM) was used (Figure 4). It is obvious from SEM photograph that the nanocomposite has a net-like structure. The wrinkles of GO sheets could easily be observed in the GO-chitosan SEM image.

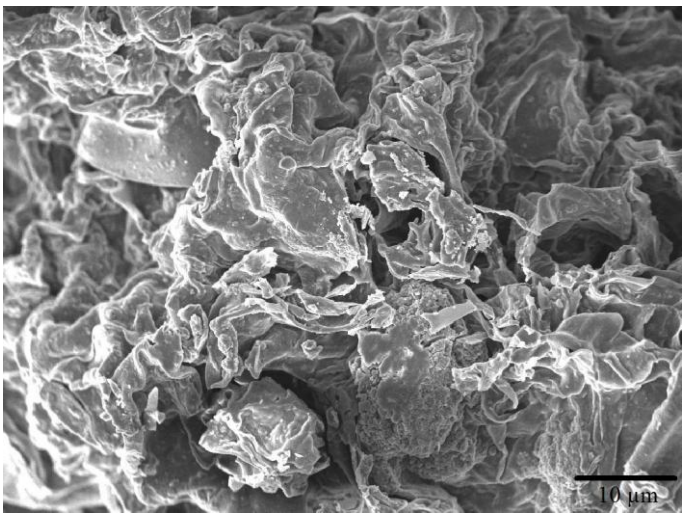

Figure 4. SEM image obtained from GO-chitosan nanocomposite

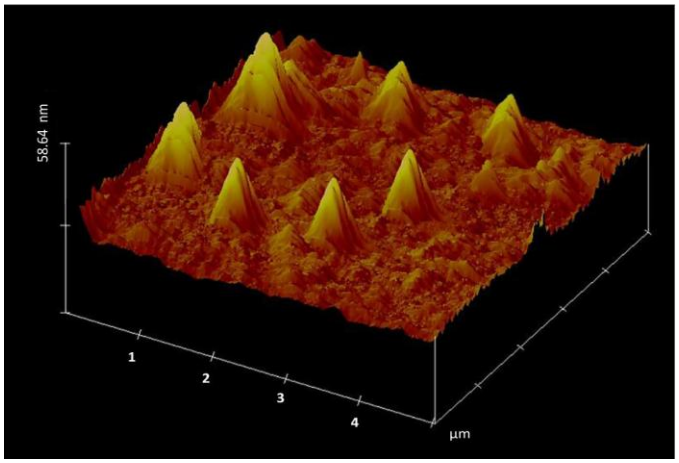

Figure 5. AFM image of GO-chitosan nanocomposite.

For the confirmation of the nanostructured surface of the catalyst also atomic force microscopy (AFM) was obtained. As shown in Figure 5, the average size distribution of GO-chitosan nanocomposite is 50 nm.

To explore the catalytic effect of GO-chitosan, a pilot experiment was carried out using the one-pot three-component reaction of benzaldehyde **1**, methyl acetoacetate **2** and urea **3**.

According to our investigations, the optimized amount of the catalyst is 15 mg and the best temperature for this method is 110 °C (Table 1, entry 6).

GO and chitosan also was used as a catalyst in the pilot experiment and the same conditions were tested for them but the results were not as good as GO-chitosan (Table 1, entries 8 and 9). Furthermore, at the time of separation, GO sticks to filter paper and consequently, reusability decreases. The color of chitosan, in some cases, is similar to the product sediment and accordingly, the catalyst is indiscernible from the product sediment and makes some difficulties in the synthesis procedures. Next, to investigate the efficiency and applicability of the catalyst in the three-component synthesis of multifunctionalized DHPMs **4a-s**, the Biginelli reaction was extended to other substituted benzaldehydes and 1,3-ketoesters at 110 °C under solvent-free conditions (Table 2). The results summarized in Table 2 clearly indicate the scope and generality of the reaction with respect to various benzaldehydes and 1,3-ketoesters. It is important to note, methyl acetoacetate give the product in high yields with short reaction times (Table 2, entries 1-12). The reaction time of some products has been compared with the literature (Table 2). For example, the reaction time of **4a** in this work is 10 min while the same product in the literature has been obtained after 20 min (entry 1).

Table 1. Optimization of conditions in the reaction of benzaldehyde **1**, 1,3-ketoesters **2** and urea **3** at 110 °C

Entry	Catalyst	Loading (mg)	Time (min)	Yield (%)
1	GO-chitosan	-	50	nil
2	GO-chitosan	1	50	trace
3	GO-chitosan	5	40	50
4	GO-chitosan	8	30	90
5	GO-chitosan	10	20	92
6	**GO-chitosan**	**15**	**10**	**95**
7	GO-chitosan	20	10	95
8	GO	15	10	88
9	chitosan	15	10	85

Table 2. Synthesis of 3,4-dihydropyrimidin-2(1*H*)-ones **4a-s** using GO-chitosan nanocatalyst under solvent-free conditions at 110 °C.

Entry	R'	R	Product	Time (min)	Isolated yield (%)	Mp (°C)
1	Me	phenyl	**4a**	10	86	213-215
2	Me	3-chlorophenyl	**4b**	35	88	249-250
3	Me	4-chlorophenyl	**4c**	40	85	209-210
4	Me	4-methoxyphenyl	**4d**	30	80	199-200
5	Me	4-methylphenyl	**4e**	45	86	220-222
6	Me	4-hydroxyphenyl	**4f**	30	83	251-252
7	Me	3-nitrophenyl	**4g**	10	89	284-258
8	Me	4-nitrophenyl	**4h**	45	82	246-246
9	Et	4-chlorophenyl	**4i**	45	80	216-217
10	Et	2-chlorophenyl	**4j**	45	83	222-224
11	Et	phenyl	**4k**	30	88	209-212
12	Et	4-methoxyphenyl	**4l**	50	75	207-209
13	Et	4-methylphenyl	**4m**	40	79	216-218
14	Et	4-hydroxyphenyl	**4n**	65	81	238-239
15	Et	3-nitrophenyl	**4o**	25	89	233-234
16	Et	4-nitrophenyl	**4p**	65	78	215-216
17	Et	2-nitrophenyl	**4q**	75	80	209-211
18	Et	2,4-dichlorophenyl	**4r**	50	76	248–250
19	Et	3-hydroxyphenyl	**4s**	45	82	187-189

A possible mechanism for the synthesis of DHPMs **4a-s** is shown in Scheme 2 [40]. The formation of *N*-acylimine intermediate **I**, which was produced by the reaction of the aldehyde with urea, is the first step, which is the key rate-determining step. This intermediate is activated by the hydrogen atoms existing in ammonia and the hydroxyl groups of GO–chitosan. Subsequently, the enol tautomer of ethyl acetoacetate attack to the imine that is sufficiently electrophilic and an open-chain ureide **II** is produced. Then, the intermediate **II** is cyclocondensed to the DHPMs **4a-s** with expulsion of water.

One of the most important reasons for choosing this active, non-toxic and eco-friendly heterogeneous nanocatalyst is its high degree of reusability. As shown in Figure 6, the GO–chitosan could be recovered and reused several times in the subsequent runs using the same recovered catalyst without a considerable loss of catalytic activity.

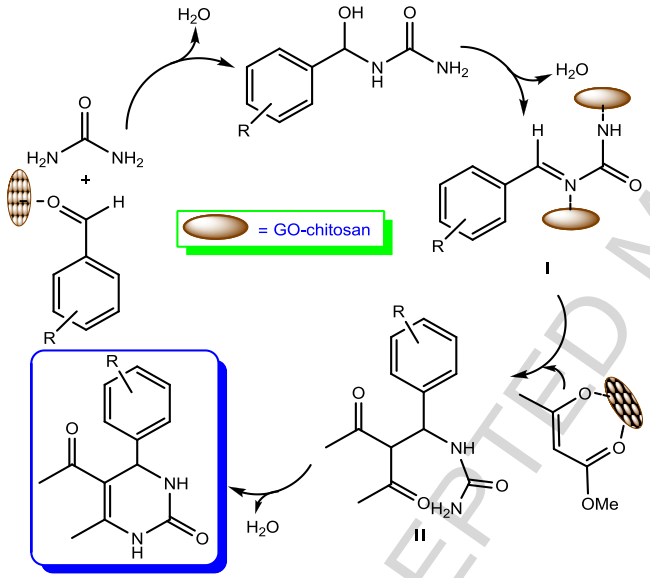

Scheme 2. Proposed mechanism for the synthesis of 3,4-dihydropyrimidin-2(1*H*)-ones **4a-s** using GO-chitosan nanocomposite.

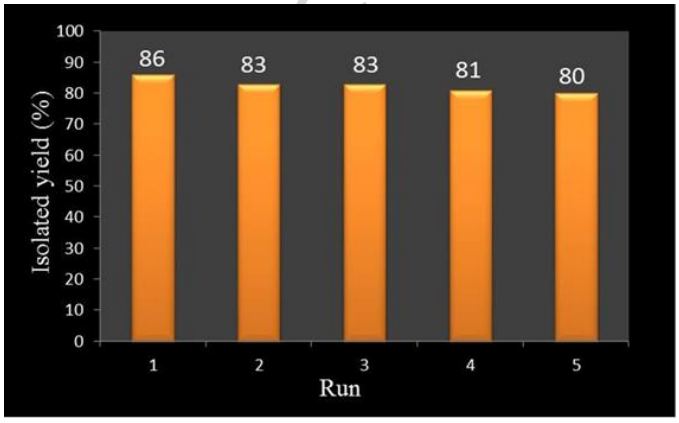

Figure 6. Reusability of GO-chitosan for synthesis of 3,4-dihydropyrimidin-2(1*H*)-one **4a-s** using GO-chitosan nanocomposite.

3. Experimental

All the solvents, chemicals and reagents were purchased from Merck, Fluka and Aldrich. Melting points were measured on an Electrothermal 9100 apparatus and are uncorrected. IR spectra were recorded on a Shimadzu IR-470 spectrometer by the method of KBr pellet. ^{1}H and ^{13}C NMR spectra were recorded on a Bruker DRX-500 Avance spectrometer at 500 and 125 MHz, respectively. The thermal properties of the samples were conducted using a thermogravimetric analyzer (TGA-DSC/Mettler Toledo) ranging from room temperature to 700 °C at a rate of 10 °C/min under N_2 atmosphere. The tip radii were obtained from direct AFM measurements of the tip apex region in tapping mode. The shell surface was mounted on the AFM stage and the Triboscope recording unit with transducers and leveling device was placed on the top of a NanoScope III E 164 | 164 mm^2 XY piezo scan base. SEM images were obtained on a Seron AIS 2100. The products were identified by comparison of their spectroscopic and analytical data with authentic samples.

3.1. Synthesis of GO

GO was prepared according to Hummers' method [41]. 40 mL H_3PO_4 (85.0%) and 360 mL of concentrated H_2SO_4 were shed into the three neck-flask charged with 2 g graphite powder under stirring conditions. 12 g $KMnO_4$ was gently added into the reaction pot that was cooled via an ice bath. The cooling bath was removed and the reaction mixture was kept at 45 °C for 48 h being sure that oxidation of graphite has been completed. The reaction mixture was quenched by 2 L of ice containing 20 mL of H_2O_2. The color of the mixture changed from dark brown to bright yellow that indicates formation of GO. The solid was gained via centrifugal separation and it washed three times with 10% HCl aqueous solution followed by distilled water until pH of 5-6 was gained. Ultimately, the resulting GO was washed with acetone and then dried at 60 °C under vacuum for 30 h.

3.2. Preparation of GO-chitosan nanocomposite

100 mg GO and 2 g chitosan were poured into a 200 mL round-bottom flask charged with 100 mL DMF. The mixture was sonicated for 1 h, 0.9 g N,N'-dicyclohexylcarbodiimide (DCC) and 0.6 g 4-dimethylaminopyridine (DMAP) were then added into the above suspension and the resulting solution was kept at room temperature for 48 h. The resulting solid was isolated by centrifugation and then washed with *ortho*-dichlorobenzene (ODCB) (3×100 mL) to remove unreacted chitosan. The mixture was subsequently washed completely with water (100 mL), methanol (100 mL) and acetone (100 mL), sequentially. Finally, it was dried at 60 °C for 24 h under vacuum conditions.

*3.3. General procedure for the synthesis of 3,4-dihydropyrimidin-2(1*H*)-ones*

The mixture of benzaldehyde (3 mmol), 1,3-ketoester (3.6 mmol), urea (4.5 mmol) was heated at 110 °C (bath temperature) in the presence of GO-chitosan (0.015 g) under solvent-free conditions. After the completion of the reaction, as indicated by TLC, the resulting reaction mixture was dissolved in 10 mL of EtOH and filtered to separate the catalyst. The filtered solution retaining product was placed in the refrigerator to obtain pure crystalline products in good-to-high yields.

3.4. Product characterization data

Methyl 4-(4-chlorophenyl)-6-methyl-2-oxo-1,2,3,4-tetrahydropyrimidine-5-carboxylate (4c): m.p.: 209–210 °C; IR (KBr) υ_{max} (cm^{-1}): 3424 (NH), 3248 (NH), 1705 (C=O), 1647 (C=O), 1223 (C–O), 1092 (C–N); ^{1}H NMR (500 MHz, $CDCl_3$): δ_H (ppm) = 2.31 (s, 3H), 3.59 (s, 3H), 5.26 (d, J = 3.5 Hz, 1H),

7.26 (m, 4H), 7.51 (s, 1H, NH), 9.11 (s, 1H, NH); ^{13}C NMR (125 MHz, $CDCl_3$); δ_C (ppm) = 18.79, 52.60, 57.70, 98.98, 121.23, 123.60, 127.58, 135.00, 142.60, 146.66, 152.62.

Ethyl 6-methyl-2-oxo-4-phenyl-1,2,3,4-tetrahydropyrimidine-5-carboxylate (4k): m.p.: 209–212 °C; IR (KBr) υ_{max} (cm^{-1}): 3424 (NH), 3235 (NH), 1705 (C=O), 1647 (C=O), 1223 (C–O), 1092 (C–N); ^{1}H NMR (500 MHz, $CDCl_3$): δ_H (ppm) = 1.07 (t, J = 7.1 Hz, CH_3), 2.15 (s, 3H, CH_3), 3.95 (q, J = 7.1 Hz, 2H, CH_2), 5.40 (s, 1H, CH), 7.25–7.33 (m, 5H, Ar–H), 7.74 (NH), 9.2 (NH); ^{13}C NMR (125 MHz, $CDCl_3$): δ_C (ppm) = 13.70, 17.79, 57.70, 63.60, 100.99, 126.23, 126.60, 127.58, 135.90, 142.60, 146.60, 152.60.

Ethyl 4-(4-methoxyphenyl)-6-methyl-2-oxo-1,2,3,4-tetrahydropyrimidine-5-carboxylate (4l): m.p.: 207–209 °C; IR (KBr) υ_{max} (cm^{-1}): 3424 (NH), 3235 (NH), 1707 (C=O), 1645 (C=O), 1225 (C–O), 1095 (C–N); ^{1}H NMR (500 MHz, $CDCl_3$): δ_H (ppm) = 1.17 (t, J = 7.1 Hz, 3H), 2.33 (s, 3H), 3.78 (s, 3H), 4.45 (q, J = 7.1 Hz, 2H), 5.41 (d, 1H), 5.65 (s, 1H, NH), 6.18 (d, J = 3.5 Hz, 2H), 7.22 (d, J = 7.1 Hz, 2H), 7.74 (s, 1H, NH), ^{13}C NMR (125 MHz, $CDCl_3$): δ_C (ppm) =14.60, 18.79, 52.60, 57.70, 60.79, 108.99, 121.23, 123.60, 127.28, 135.00, 142.60, 146.60, 162.60.

Ethyl 4-(4-methylphenyl)-6-methyl-2-oxo-1,2,3,4-tetrahydropyrimidine-5-carboxylate (4m): m.p.: 216–218 °C; IR (KBr) υ_{max} (cm^{-1}): 3421 (NH), 3234 (NH), 1709 (C=O), 1646 (C=O), 1227 (C–O), 1095 (C–N); ^{1}H NMR (500 MHz, $CDCl_3$): δ_H (ppm) = 1.17 (t, J = 7.1 Hz, 3H), 1.97 (s, 3H), 2.33 (s, 3H), 4.07 (q, J = 7.1 Hz, 2H), 5.41 (d, J = 3.5 Hz, 1H), 5.65 (s, 1H, NH), 6.18 (d, J = 7.1 Hz, 2H), 7.25 (d, J = 7.1 Hz, 2H), 7.74 (brs, 1H, NH); ^{13}C NMR (125 MHz, $CDCl_3$): δ_C (ppm) =14.00, 15.99, 52.50, 57.75, 60.79, 105.09, 121.53, 123.65, 127.58, 135.50, 140.60, 146.60, 160.65.

Ethyl 4-(4-hydroxyphenyl)-6-methyl-2-oxo-1,2,3,4-tetrahydropyrimidine-5-carboxylate (4n): m.p.: 238–239 °C; IR (KBr) υ_{max} (cm^{-1}): 3586 (OH), 3428 (NH), 3233 (NH), 1713 (C=O), 1649 (C=O), 1220 (C–O), 1092 (C–N); ^{1}H NMR (500 MHz, $CDCl_3$): δ_H (ppm) = 1.79 (t, J = 7.1 Hz, 3H, CH_3), 3.94 (q, J = 7.1 Hz, 2H, CH_2), 5.40 (s, 1H, CH), 7.25–7.33 (m, 5H, Ar–H), 7.74 (NH), 9.20 (NH), 9.40 (OH); ^{13}C NMR (125 MHz, $CDCl_3$): δ_C (ppm) = 13.50, 17.79, 57.70, 63.60, 100.99, 117.58, 126.60, 127.58 135.90, 142.60, 146.60, 152.60.

Ethyl 4-(3-nitrophenyl)-6-methyl-2-oxo-1,2,3,4-tetrahydropyrimidine-5-carboxylate (4o): m.p.: 233–234 °C; IR (KBr) υ_{max} (cm^{-1}): 3424 (NH), 3235 (NH), 1705 (C=O), 1647 (C=O), 1223 (C–O), 1092 (C–N); ^{1}H NMR (500 MHz, $CDCl_3$): δ_H (ppm) = 1.09 (t, J = 7.1 Hz, 3H), 2.16 (s, 3H, CH_3), 3.94 (q, J = 7.1 Hz, 2H, CH_2), 6.12 (d, J = 3.4 Hz, 1H), 7.16–7.33 (m, 5H, Ar–H), 7.74 (NH), 9.2 (NH); ^{13}C NMR (125 MHz, $CDCl_3$): δ_C (ppm) = 14.00, 15.99, 52.50, 60.79, 105.09, 121.53, 123.65, 127.58, 132.00, 132.50, 135.50, 140.60, 146.60, 160.65.

4. Conclusion

In summary, we have introduced GO-chitosan nanocomposite as a biocompatible and biodegradable heterogeneous nanocatalyst applicable in the organic synthesis. Then, efficient synthesis of 3,4-dihydropyrimidin-2(1*H*)-one were carried out starting from simple and readily available precursors including benzaldehydes, 1,3-ketoesters and urea in the presence of a catalytic amount of GO-chitosan under solvent-free conditions. A large number of unique properties in this catalyst have caused to short reaction time, easy work-up procedure, high reusability of the nanocatalyst, high atom economy, excellent yields and environmentally benign reaction conditions. In addition, to the best of our knowledge, this is the first report of using this nanocomposite in the synthesis of DHPMs via MCRs.

Acknowledgements

The authors gratefully acknowledge the partial support from the Research Council of the Iran University of Science and Technology.

Supporting Information

Electronic Supplementary Information includes copies of the ^{1}H and ^{13}C NMR analysis of the prepared products.

References

[1] Dömling, A.; Wang, W.; Wang, K. *Chem. Rev*. **2012**, *112*, 3083.
[2] Mayer, T. U.; Kapoor, T. M.; Haggarty, S. J.; King, R. W.; Schreiber, S. L.; Mitchison, T. J. *Science* **1999,** *286*, 971.
[3] Maliga, Z.; Kapoor, T. M.; Mitchison, T. J. *Chem. Biol*. **2002**, *9*, 989.
[4] Timoshenko, V. M. *Arkivoc* **2014**, *6*, 86.
[5] Zhang, Q.; Wang, X.; Li, Z.; Wu, W.; Liu, J.; Wu, H.; Cui, S.; Guo, K. *RSC Adv*. **2014**, *4*, 19710.
[6] Kolvari, E.; Koukabi, N.; Armandpour, O. *Tetrahedron* **2014**, *70*, 1383.
[7] Karthikeyan, P.; Aswar, S. A.; Muskawar, P. N.; Bhagat, P. R.; Senthil Kumar, S. *J. Org. Chem.* **2013**, *723*, 154.
[8] Shockravi, A.; Kamali, M.; Sharifi, N.; Nategholeslam, M.; Moghanlo, S. P. *Synth. Commun*. **2012**, *4*, 1477.
[9] Safari, J.; Gandomi-Ravandi, S. *J. Mol. Struct*. **2014**, *1065–1066*, 241.
[10] Qiu, Y.; Sun, H.; Ma, Z.; Xia, W. *J. Mol. Catal. A: Chem*. **2014**, *392*, 76.
[11] Narkhede, N.; Patel, A. *J. Por. Mater*. **2014**, *21*, 579.
[12] Xu, Z.; Jiang, Y.; Zou, S.; Liu, Y. *Phosphorus, Sulfur Silicon Relat. Elem.* **2014**, *189*, 791.
[13] Jetti, S. R.; Upadhyaya, A.; Jain, S. *Med. Chem. Res*. **2014**, *23*, 4356.
[14] Jetti, S. R.; Bhatewara, A.; Kadre, T.; Jain, S. *Chin. Chem. Lett*. **2014**, *25*, 469.
[15] Zarnegar, Z.; Safari, J. *J. Nanopart. Res.* **2014**, *16*, 2509.
[16] Jadhav, S.; Anandgaonker, P. L.; Kulkarni, G.; Gaikwad, S. T.; Rajbhoj, A. S. *J. Cluster Sci*. **2014**, *25*, 1389.
[17] Prakash, G. K. S.; Lau, H.; Panja, C.; Bychinskaya, I.; Ganesh, S. K.; Zaro, B.; Mathew, T.; Olah, G. A. *Catal. Lett.* **2014**, *144*, 2012.
[18] Pramanik, M.; Bhaumik, A. *ACS Appl. Mater. Interfaces* **2014**, *6*, 933.
[19] Kiyani, H.; Ghiasi, M. *Res. Chem. Intermed*. **2014**, DOI: 10.1007/s11164-014-1766-7.
[20] Thorat, P. B.; Waghmode, N. A.; Karade, N. N. *Tetrahedron Lett.* **2014**, *55*, 5718.
[21] Safari, J.; Zarnegar, Z. *RSC Adv*. **2013**, *3*, 17962.
[22] Wang, A.; Liu, X.; Su, Z.; Jing, H. *Catal. Sci. Tech.* **2014**, *4*, 71.
[23] Poliakoff, M.; Licence, P. *Nature* **2007**, *450*, 810.
[24] Maleki, A.; Paydar, R. *RSC Adv*. **2015**, *5*, 33177.
[25] Maleki, A.; Movahed, H.; Paydar, R. *RSC Adv.* **2016,** *6*, 13657.
[26] Maleki, A. *Tetrahedron* **2012**, *68*, 7827.
[27] Maleki, A. *Tetrahedron Lett.* **2013**, *54*, 2055.
[28] Maleki, A.; Kamalzare, M. *Catal. Commun.* **2014**, *53*, 67.
[29] Maleki, A.; Akhlaghi, E.; Paydar, R. *Appl. Organomet. Chem.* **2016,** *30*, 382.
[30] Marcano, D. C.; Kosynkin, D. V.; Berlin, J. M.; Sinitskii, A.; Sun, Z.; Slesarev, A.; Alemany, L. B.; Lu, W.; Tour, J. M. *ACS Nano* **2010,** *4*, 4806.
[31] El-Kady, M. F.; Kaner, R. B. *ACS Nano* **2014,** *8*, 8725.
[32] Shao, Y.; Wang, J.; Wu, H.; Liu, J.; Aksay, I. A.; Lin, Y. *Electroanalysis* **2010,** *22*, 1027.
[33] Dhand, V.; Rhee, K. Y.; Ju Kim, H.; Ho Jung, D. *J. Nanomaterial* **2013,** DOI: 10.1155/2013/763953.
[34] Kucinskis, G.; Bajars, G.; Kleperis, J. *J. Power Sources* **2013,** *240*, 66.
[35] Zhang, X.; Zhang, H.; Li, C.; Wang, K.; Sun, X.; Ma, Y. *RSC Adv.* **2014,** *4*, 45862.
[36] Cataldo, S.; De Stefano, C.; Gianguzza, A.; Piazzese, D.; Sammartano, S. *Chem. Spec. Bioavailab*. **2009,** *21*, 81.

[37] Cataldo, S.; Crea, F.; Gianguzza, A.; Pettignano, A.; Piazzese, D. *J. Mol. Liq.* **2009,** *148*, 120.
[38] Ravi Kumar, M. N. V. *React. Funct. Polym.* **2000,** *46*, 1.
[39] Zuo, P. P.; Feng, H. F.; Xu, Z. Z.; Zhang, L. F.; Zhang, Y. L.; Xia, W.; Zhang, W. Q. *Chem. Cent. J.* **2013**, *7*, 39.
[40] Kappe, C. O. *J. Org. Chem.* **1997,** *62*, 7201.
[41] Hummers, W. S; Offeman, R. E. *J. Am. Chem. Soc.* **1958**, *80*, 1339.

Bionanostructure-catalyzed one-pot three-component synthesis of 3,4-dihydropyrimidin-2(1H)-one derivatives under solvent-free conditions

Ali Maleki* and Reza Paydar

Catalysts and Organic Synthesis Research Laboratory, Department of Chemistry, Iran University of Science and Technology, Tehran 16846-13114, Iran

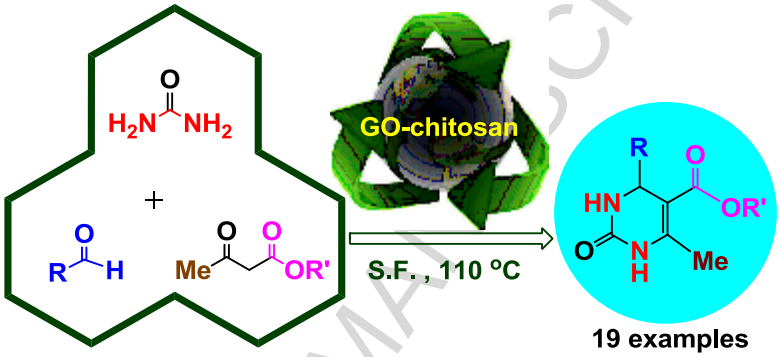

Graphical abstract

Highlights

- An environmentally benign biopolymer-based nanocomposite was prepared.
- It was characterized by FT-IR, TGA, DSC, SEM and AFM analyses.
- The first use of this nanocatalyst in the synthesis of dihydropyridinones.
- The products were obtained in high atom economy and easy work-up procedure.